

Generation of Digital Elevation Models from Sentinel-1 Datasets and Suitability Assessment for Further Use: A Case Study of Melamchi Watershed

Sushil Pokhrel ^a, Umesh Singh ^b, Pawan Kumar Bhattarai ^c, Ananta Man Singh Pradhan ^d

^{a, c} Department of Civil Engineering, Pulchowk Campus, IOE, Tribhuvan University, Nepal

^b Hydro Lab Pvt. Ltd., Lalitpur, Nepal

^d Ministry of Energy, Water Resources and Irrigation, Water Resources Research and Development Centre, Government of Nepal, Pulchowk, Lalitpur 44700, Nepal

✉ ^a sushil.pokhrel.100@gmail.com

Abstract

Digital Elevation Model (DEM) represent the continuous variation of earth topography and is main input for wide range of geospatial applications. Mass wasting processes which are frequent in mountainous regions change the landforms of the area. Continuously updated DEMs are thus required for reliable estimates of volume of sediments associated with such events. In this research, we generated DEMs from Sentinel-1 SAR datasets and assessed their suitability for estimation of sediment volumes associated with mass wasting event that occurred in upper parts of Melamchi watershed on 15 June, 2021. The pre and post event DEMs generated using image pairs from ascending and descending flight directions and two orbit tracks showed high difference in elevation range for the same spatial extent and are thus unsuitable for DEMs of Difference technique for volume estimation without further post-processing since DEM generation from Sentinel-1 datasets are influenced by many factors.

Keywords

DEM, InSAR, mass wasting, Melamchi, Nepal, perpendicular baseline, SAR, sediment volume, Sentinel-1, SNAP, temporal baseline

1. Introduction

Digital Elevation Model (DEM) is the three dimensional representation of terrain elevation. They depict the continuous variations of the Earth's topography, mostly stored within cells of a regular raster grid, and are the main input for a large variety of applications, including geomorphologic mapping of landforms, numerical modeling of hydrologic processes, watershed and visibility computations, and many other forms of spatial analyses incorporating three or more dimensions[1].

In mountainous terrain, mass-wasting processes dominate landscape evolution posing risk to life and socioeconomic development[2]. The estimation of sediment volumes associated with such processes is key parameter for hazard analysis. Among numerous methods for estimating the volume, the DEMs of Difference (DoD) technique with the use of pre and post-event DEMs is a good estimator. However,

accurate representation of topographical variation though DEMs on either side of an event is rarely available. In fact, such mass wasting processes often occur in remote areas with difficult terrain, making the field visit and data collection immediate aftermath very challenging. Thus the straight forward generation of post-event DEMs based on freely available data is very important[3]. While the information of sediment volume associated with such event defines the magnitude of the disaster, reliable data on volume of sediments released from the source area and spatial distribution of sediments in deposition area serve as input and validation parameters for mass flow simulation tools.

DEM can be generated from ground topographical surveys(conventional), Global Navigation Satellite Systems, stereophotogrammetry, structure from-motion, Light Detection and Ranging (LiDAR), Interferometric Synthetic Aperture Radar(InSAR) technique, etc. Among these techniques,

stereophotogrammetry and InSAR can be used to generate DEMs exploiting continuously updated and freely available remote sensing data. ASTER GDEM, a widely used global DEM product was generated from millions of optical images of earth's surface taken between 2001 to 2007 using stereophotogrammetry[4]. Another global DEM product, SRTM which is fairly comparable to ASTER GDEM in terms of spatial resolution as well as its popularity among users was generated from Interferometric Synthetic Aperture Radar (InSAR) technique using SAR imageries of earth's surface taken over 11 days mission in 2000 A.D.[5]. Though easily available, their spatial resolution of 30m make them unsuitable for many applications. Like wise, as they were generated from image acquisition of earth's surface long ago, they do not depict the topography of earth as it is now.

Optical (passive) sensors are unable to acquire images of Earth surface through the clouds and to operate without daylight while active, "all-weather" and "day-and-night", microwave radar sensors are capable of cloud penetration and of working independent of sun[6]. This gives the products derived from radar data edge over those derived from optical data, especially in places of Nepal, where such events are triggered during monsoon period and the places are under thick cloud cover during and right after events.

In this study, we focus on mass wasting event that occurred on 15 June 2021 on headwaters region of Melamchi Watershed, situated on north central part of Nepal with the purpose of assessing the quality of DEMs generated from freely available SAR data with InSAR procedure for estimation of sediment volumes associated with mass wasting processes in high altitude mountainous region. The specific objectives of the study are:

- i) To generate pre and post event DEMs from freely available Sentinel-1 datasets and
- ii) To assess the suitability of those DEMs for use in DEMs of Difference (DoD) procedure.

2. Methodology

2.1 Study Area

The study area lies at the upper part of Melamchi River Catchment, in particular the part of the catchment upstream of the old landslide dam at Bhemathang (Figure 1). The area is located south of

Langtang Mountain Range of Nepal Himalayas at north central part of Nepal. Within the study area two streams, Melamchi flowing in the left and Pemdán flowing in the right merge at Bhemathang area, a wide river valley which used to be braided with very gentle slope before the June 15th event. The river formed by the confluence of two streams is again known as Melamchi and flows downstream of old landslide dam in south direction. The lowest elevation of Bhemathang area before the event was 3566 masl while the peak elevation of Melamchi stream catchment reaches 5916 masl and that of Pemdán stream catchment reaches 5832 masl.

On the evening of 15 June 2021, catastrophic sediment and flood disaster hit Melamchi watershed. Pemdán and Melamchi streams at the upper part of Melamchi catchment transported sediments to the Bhemathang braid plain forming large deposition area of about 0.81 km^2 . On Pemdán catchment, two distinct sediment source area at mid region are visible. The right source area lies at the end of moraine dammed lake while the left one lies on the principal flow path of Pemdán stream. During the 6 day period from June 9 to June 14, 2021 the area received more than 200 mm of rainfall, while the area had already received about 129% more rainfall than the average rainfall for March to May pre-monsoon period[7] contributing to the sediment disaster of such scale. Figure 2 shows the deposition area at Bhemathang viewed downstream where Pemdán stream flows from bottom right to centre left and joins Melamchi stream flowing from bottom left to top left.

2.2 Data and Tools

Sentinel-1 Single Look Complex (SLC) Terrain Observation with Progressive Scans Synthetic Aperture Radar (TOPSAR) datasets from Sentinel-1 mission have been used in this study for generation of DEMs using InSAR procedure. Sentinel-1, the C-band radar mission (wavelength of 5.6 cm) within Copernicus Programme of European Space Agency (ESA) constituted of Sentinel-1A (S1A) and Sentinel-1B (S1B) until the end of S1B on August, 2022 and provided an unprecedented amount of open source data with 12 days revisit time for each satellite and 6 days revisit time when the satellites worked in tandem. The quality of the DEMs generated by InSAR procedure depends upon the perpendicular and temporal baseline between the two images used. Perpendicular baseline is the component of spatial

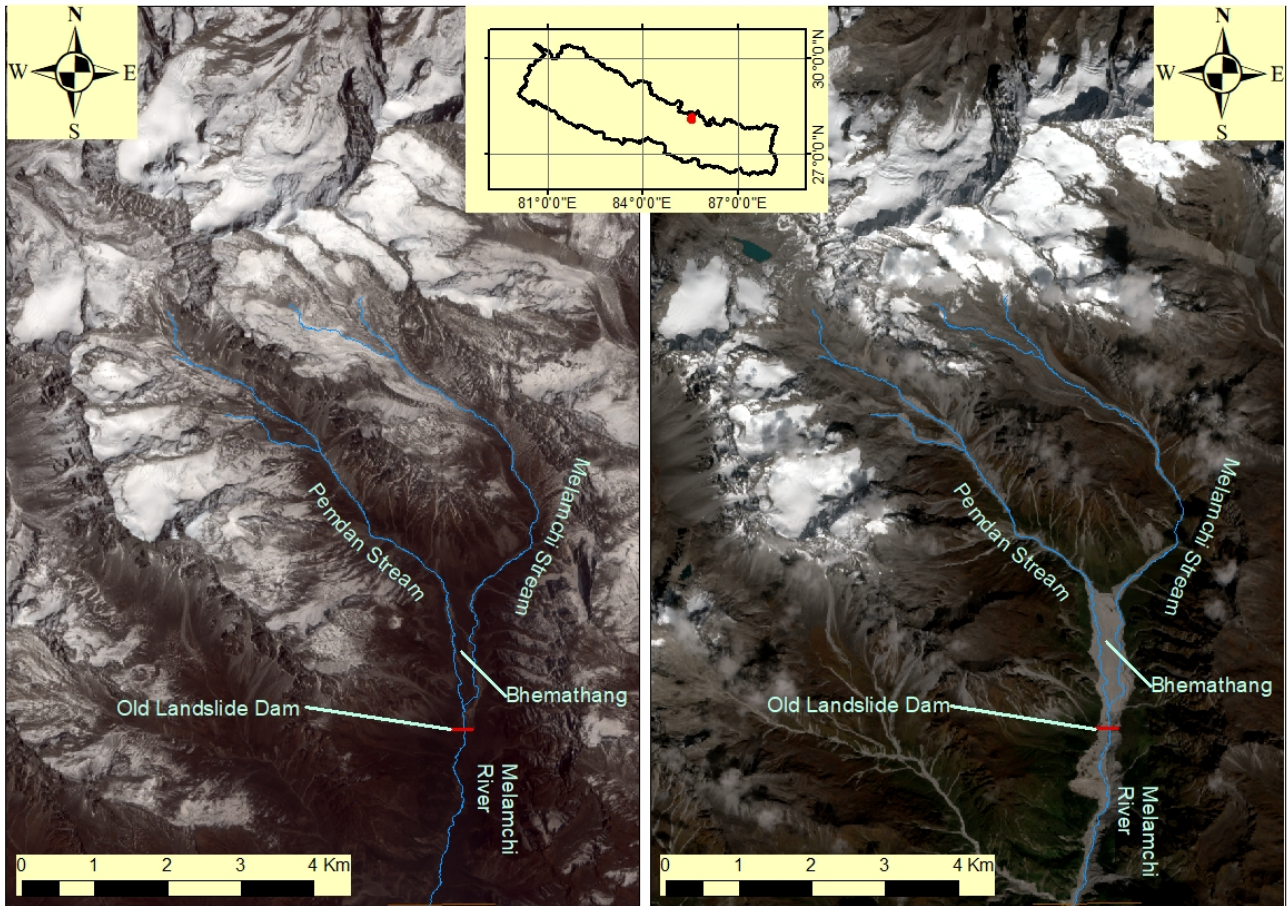


Figure 1: The study area on the headwaters region of Melamchi River Catchment. Sentinel-2 image on left shows the pre-event topography of the area acquired on April 05, 2021 while Sentinel-2 the image on right shows the post-event topography acquired on October 12, 2021. The red spot in the inset map on top centre shows the location of the study area in Nepal.



Figure 2: Deposition area at Bhemathang viewed from upstream towards downstream. (Image courtesy: www.ekantipur.com)

baseline in perpendicular direction between the location of radar antenna during two acquisitions. If perpendicular baselines are too small, the differential phase do not show pronounced change in topography. Meanwhile, too large perpendicular baseline make the coherent phase increasingly different, leading to decorrelation. Recommended suitable B_{perp} for DEM generation using ERS satellite product is between 150-300 m. However, a lower range of B_{perp} have generally been used for Sentinel-1 data. Dabiri et. al., 2021 [3] used B_{perp} values between 134 and 159m for DEM generation using Sentinel-1 data.

On the other hand, the time interval between the acquisitions of two images (temporal baseline) should be kept as short as possible to lessen the temporal decorrelation of phase. Because of its relatively short wave length, C-band radar of Sentinel-1 is prone to temporal decorrelation.

Alaska Satellite Facility (ASF) Baseline tool was used

for identification and selection of image pairs. Images from two orbit tracks (number 19 and number 85) and both ascending and descending flight directions were used in the search of image pairs, from which one pre-event Sentinel-1A image pair and three post-event Sentinel-1A image pairs were selected (Table 1). InSAR stack overview function available in Sentinel Application Platform (SNAP) toolbox was used to work out the modeled coherency, and the height ambiguity between two TOPSAR pair images. There were minor discrepancies in perpendicular baseline values given by ASF Baseline tool and InSAR stack overview function of SNAP toolbox, the value given by InSAR stack overview function of SNAP toolbox have been used in the study.

All processing works were accomplished using the open-source SNAP toolbox developed by ESA. Besides, SRTM 1secHGT DEM freely accessible within SNAP tool box was used as reference DEM for generation process.

2.3 DEM Generation

DEMs constitute important input parameter for mass flow modelling, extraction of topographic information (slope, relief, aspect) and volumetric calculation associated with event involving sediment transportation. In this study we explored the straight forward and automated DEM generation workflow using the Sentinel-1 SLC TOPSAR datasets and InSAR procedure and then assessed the suitability of the generated DEMs for further uses. One pair of pre event TOPSAR images and three pairs of post event TOPSAR images were selected with due consideration to spatial and temporal baseline values. Interferometric synthetic aperture radar (InSAR) exploits the phase difference between two complex SAR images taken from slightly different sensor positions and extracts information about the earth's surface [8]. The workflow for generation of DEM from SLC TOPSAR images include basic steps of TOPS Split, which decreases the SLC data to single sub-swath and bursts covering only the area of interest, then coregistration by Back Geocoding and Enhanced Spectral Diversity (ESD), and then the formation of interferogram including removal of phase contribution of flat earth surface (ϕ_{flat}) in total phase. The unwrapping of phase is done outside SNAP by independently licensed tool snaphu (statistical-cost network-flow algorithm for phase unwrapping [9]) which is then imported back to

SNAP toolbox and translated into metric units based on an external reference DEM [10] and geocoded using Range Doppler terrain correction. Details on the process of DEM generation from Sentinel-1 data along with number of potential sources of error and limitations are provided in Braun, 2020 [8].

In this study, four image pairs along track number 19 (Table 1), first sub-swath and bursts 6 & 7 were used in TOPS Split while for image pair along track number 85, second sub-swath and bursts 3 & 4 were used. SRTM 1SecHGT DEM was used during the interferogram formation. The phase unwrapping was done by statistical-cost network-flow algorithm for phase unwrapping (snaphu) tool outside SNAP and imported back into SNAP. Then the phase was translated into elevation information based on the same SRTM 1SecHGT DEM as reference DEM. Finally, the generated DEM was geocoded using Range Doppler terrain correction available in SNAP.

2.4 Validation

The generated DEMs were assessed for accuracy by using high resolution 4.4 m DEM. Literatures [3, 11] recommend that resolution of the reference data be at least three times higher than the resolution of DEM being evaluated. Statistical measures such as the minimum, maximum, mean, and standard deviation of elevations values of the generated DEMs and that of reference DEM were compared to assess the quality of derived DEMs. The vertical quality assessment was completed using the root mean square error (RMSE).

The RMSE contain both random and systematic errors introduced during data production [12], and is expressed by the equation 1 as:

$$RMSE = \sqrt{\frac{\sum (y_i - y_{ti})^2}{N}} \quad (1)$$

where y_i refers to the i th interpolated elevation, y_{ti} refers to the i th known or measured elevation of a sample point in a reference dataset, and N is the number of sample points.

3. Results and Discussion

3.1 DEM Generation

One pre-event DEM and three post-event DEMs were created from Sentinel-1 SLC TOPSAR datasets using InSAR procedure. Figure 3 shows the DEMs

Table 1: Sentinel-1 datasets and their characteristics used for the generation of Digital Elevation Models (DEMs)

Sentinel-1 Pairs	Image	Orbit Track	Flight Direction	Temporal Baseline (days)	Bperp (m)	Modeled Coherency	Height Ambiguity	Pre-/Post-event
3 May 2021 and 27 May 2021		19	Descending	24	149	0.86	105.15	Pre
24 June 2021 and 28 September 2021		85	Ascending	96	154	0.79	102.11	Post
26 July 2021 and 07 August 2021		19	Descending	12	118	0.89	132.29	Post
31 August 2021 and 23 November 2021		19	Descending	84	148	0.81	105.86	Post

generated from image pairs of different orbit tracks, and the pre-event high resolution DEM used for comparison. High discrepancy in the range of elevation values for same area is clearly visible. All of the DEMs give higher minimum elevation value and lower maximum elevation value than that of reference DEM, resulting in lower elevation range for all DEMs generated compared to reference DEM. As a result, the standard deviation of elevation values for all the DEMs generated are lower than that of reference DEM (Table 2). The study area lies in mountainous region consisting numerous ridges and river valleys, higher standard deviation of elevation values like that of reference DEM better representing the topography. Higher minimum elevation values and lower mean elevation values for all the DEMs suggest that majority of raster pixels of generated DEMs have picked elevation values in lower range, failing to capture the higher elevations and steep topography of the region.

The DEM generated from image pair of 26 July and 07 August 2021 shows best resemblance with reference DEM in terms of visual evidence as well as statistical parameters from among the suits of DEMs generated (Figure 3 and Table 2). The image pair had the least temporal baseline. Interestingly, the DEM generated from image pair of June 24 and 28 September 2021, with largest value of temporal baseline has severely underestimated the elevation range. To achieve a good vertical accuracy, the SAR image pair require a large B_{perp} [10]. The Sentinel-1 image pairs with high perpendicular baseline values in the range of 150m - 300m were extremely hard to find for the study area. Thus, in order to ensure the B_{perp} between the two image pair was as high as possible, image pairs with temporal baselines higher than 12 days, the revisit time of Sentinel-1 for regions of

Nepal were also included in the study. The severe underestimation of elevation range of the area by the DEM generated from image pair of June 24 and 28 September can be attributed to higher temporal baselines, as C-band Sentinel-1 datasets are susceptible to temporal phase decorrelation.

Apart from perpendicular and spatial baselines, the atmospheric condition, vegetation cover and direction of flight (ascending or descending) also alter the vertical accuracy of DEMs generated from Sentinel-1 datasets using InSAR procedure [1]. The image pair of June 24 and September 28 were taken along ascending flight direction while all other image pairs were taken along descending flight direction. From the result of DEM generation, the study area is found to be mapped favourably from descending track of Sentinel-1. Although radar imagery is known for its all-weather measurement capability, changes in the atmospheric conditions (mainly water vapor) cause a variable path delay which results in atmospheric distortions and is the main error source in repeat-pass SAR interferometry [13]. Due to lack of image pairs with B_{perp} in the range recommended for generation of DEMs from interferometry process, we could not exclude the SAR images acquired during the period of known high atmospheric water content for the region, and the image pairs included in the study were the best datasets available taking all selection criteria into consideration.

3.2 DEM Validation

The RMSE error for all of the generated DEMs are on significantly higher side as shown in Table 2. The lowest RMSE value is obtained for DEM generated from the image pair of July 26 2021 and August 07 2021 with RMSE value of 290.90 m. In comparison

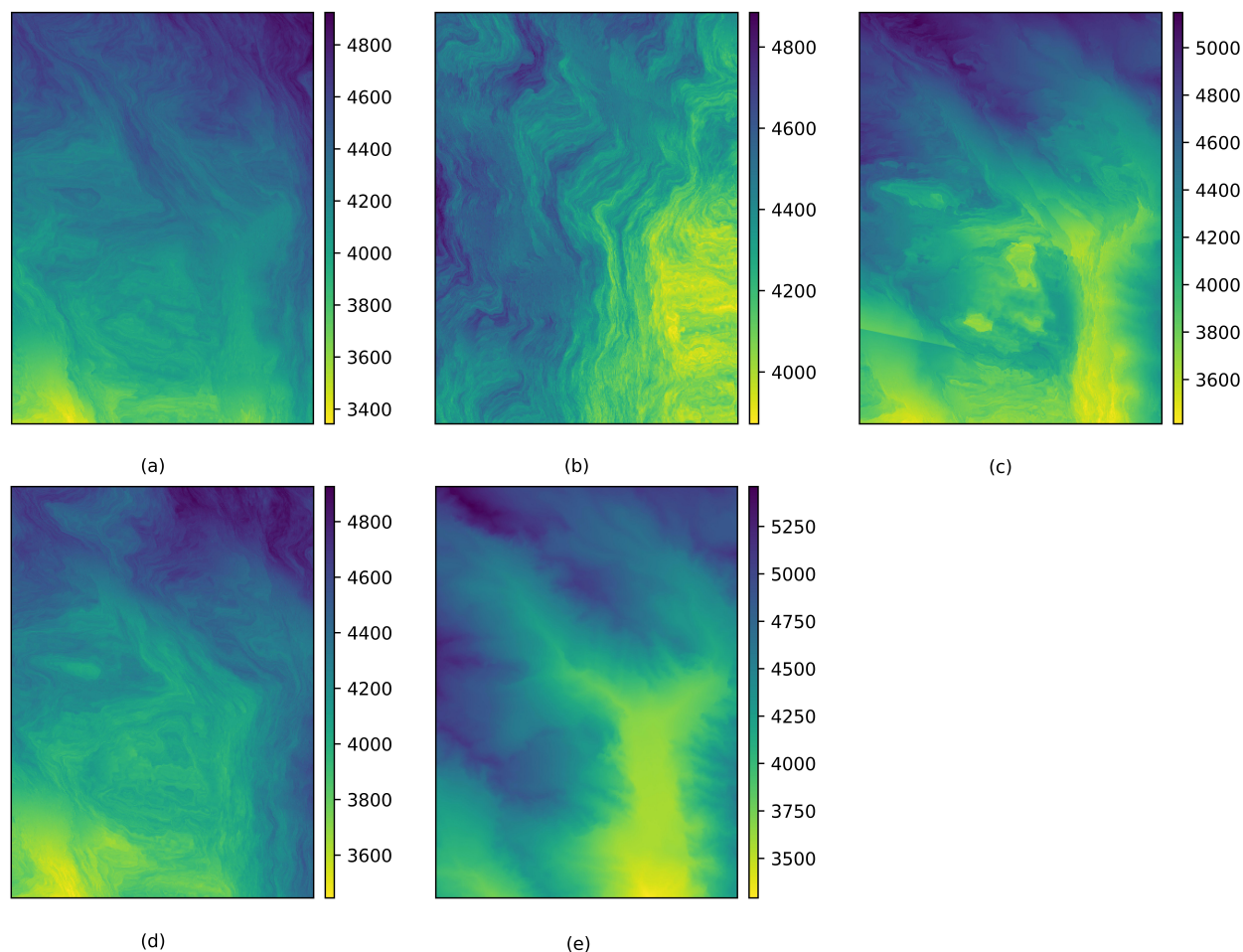


Figure 3: Illustration of DEMs generated from Sentinel 1 image pairs a) for 3 May 2021 and 27 May 2021 b) for 24 June 2021 and 28 September 2021 c) for 26 July 2021 and 7 August 2021 d) for 31 August 2021 and 23 November 2021 e) 4.4 m resolution reference DEM

to 30m resolution ASTER GDEM which was found to have RMSE of 8.53 for conterminous United States[14] and SRTM which has RMSE of 9.72 at global scale[15], the RMSE values obtained from the generated DEMs are very high. The high RMSE error value of 290.90 m for DEM generated from image pairs of 26 July 2021 and 07 August 2021 too, which predicted the elevation values nearest to that of reference DEM in terms of minimum and maximum elevation, shows that even though the range of elevation values for generated DEM is closer to that of reference DEM, there is very high difference in the elevation values of each pixels between the generated and reference DEMs.

4. Conclusion

Mass wasting processes like June 15 2021 event on Melamchi watershed change the landforms, making

the suitability assessment studies of creation of DEMs from Sentinel-1 datasets relevant. Straight forward workflow for generation of DEMs using Sentinel-1 image pairs from two different tracks was applied in this study.

Our study suggest that generation of DEMs from Sentinel-1 datasets has several limitation. The criteria of high perpendicular baselines, low temporal temporal baselines and suitable atmospheric conditions are extremely hard to meet, especially in the regions with high revisit time of 12 days for the Sentinel-1 satellite, which adversely affect the quality of DEMs obtained. Sentinel-1 was mainly designed for retrieval of surface deformations using differential InSAR (DInSAR) which requires very low B_{perp} value, and DEM generation was not the primary goal of the mission[16].

The statistics in Table 2 show that none of the DEMs

Table 2: Statistics used for validation of DEMs generated from SAR image pairs with the reference DEM. Comparison is based on area not affected by debris flow.

Image Pairs	Min Elevation (m)	Max Elevation(m)	Mean Elevation (m)	Std. Dev (m)	RMSE (m)
Reference DEM					
-	3291	5460	4400.01	457.29	-
Pre-event DEM					
3 May 2021 and 27 May 2021	3343.47	4924.18	4242.59	273.30	394.59
Post-event DEM					
June 24 2021 and 28 September 2021	3872.29	4885.05	4368.35	192.51	331.01
26 July 2021 and 07 August 2021	3412.87	5148.69	4247.97	392.74	290.92
31 August 2021 and 23 November 2021	3445.94	4925.74	4238.78	290.12	405.61

generated are suitable for further use in volumetric calculation. No post processing procedures were used in order to increase the quality of generated DEMs as this research was the suitability assessment study of DEMs generated from open source Sentinel-1 imageries.

Acknowledgments

The authors are thankful to Water Resources Research and Development Center (WRRDC) for supporting the research through “Project/Thesis Interns And Researcher Mobilization Program (SN: 11.5.40.89)”.

References

- [1] Andreas Braun. Retrieval of digital elevation models from sentinel-1 radar data—open applications, techniques, and limitations. *Open Geosciences*, 13(1):532–569, 2021.
- [2] Joshua N Jones, Sarah J Boulton, Martin Stokes, Georgina L Bennett, and Michael RZ Whitworth. 30-year record of himalaya mass-wasting reveals landscape perturbations by extreme events. *Nature communications*, 12(1):1–15, 2021.
- [3] Zahra Dabiri, Daniel Hölbling, Lorena Abad, Jón Kristinn Helgason, Þorsteinn Sæmundsson, and Dirk Tiede. Assessment of landslide-induced geomorphological changes in hítardalur valley, iceland, using sentinel-1 and sentinel-2 data. *Applied Sciences*, 10(17):5848, 2020.
- [4] ASTER NASA. Global Digital Elevation Model (GDEM); 2019. <https://lpdaac.usgs.gov/products/astgtmv003/>. Accessed: 2022-08-30.
- [5] Bernhard Rabus, Michael Eineder, Achim Roth, and Richard Bamler. The shuttle radar topography mission—a new class of digital elevation models acquired by spaceborne radar. *ISPRS journal of photogrammetry and remote sensing*, 57(4):241–262, 2003.
- [6] John R Jansen. *Introductory Digital Image Processing: A Remote Sensing Perspective*, 4th ed. Pearson Education, New York City, 2016.
- [7] SB Maharjan et al. The melamchi flood disaster: Cascading hazard and the need for multihazard risk management. 2021.
- [8] Andreas Braun. DEM generation with Sentinel-1: Workflow and Challenges, 2020.
- [9] Richard M Goldstein and Charles L Werner. Radar interferogram filtering for geophysical applications. *Geophysical research letters*, 25(21):4035–4038, 1998.
- [10] Mark A Richards. A beginner’s guide to interferometric sar concepts and signal processing [aess tutorial iv]. *IEEE Aerospace and Electronic Systems Magazine*, 22(9):5–29, 2007.
- [11] Joachim Höhle and Michael Höhle. Accuracy assessment of digital elevation models by means of robust statistical methods. *ISPRS Journal of Photogrammetry and Remote Sensing*, 64(4):398–406, 2009.
- [12] Suzanne P Wechsler. Perceptions of digital elevation model uncertainty by dem users. *URISA-WASHINGTON DC-*, 15(2):57–64, 2003.
- [13] Urs Wegmüller, Maurizio Santoro, Charles Werner, Tazio Strozzi, Andreas Wiesmann, and Wolfgang Lengert. Dem generation using ers–envisat interferometry. *Journal of Applied Geophysics*, 69(1):51–58, 2009. Advances in SAR Interferometry from the 2007 Fringe Workshop.
- [14] D Gesch, M Oimoen, J Danielson, and David Meyer. Validation of the aster global digital elevation model

version 3 over the conterminous united states. *The International Archives of Photogrammetry, Remote Sensing and Spatial Information Sciences*, 41:143, 2016.

- [15] Manas Mukul, Vinee Srivastava, Sridevi Jade, and Malay Mukul. Uncertainties in the shuttle radar topography mission (srtm) heights: Insights from the indian himalaya and peninsula. *Scientific Reports*,

7(1):1–10, 2017.

- [16] D Geudtner, P Prats, N Yague-Martinez, I Navas-Traver, I Barat, and R Torres. Sentinel-1 SAR Interferometry Performance Verification. In *Proceedings of EUSAR 2016: 11th European Conference on Synthetic Aperture Radar*, pages 1–4, 2016.